ChemComm

COMMUNICATION

View Article Online
View Journal | View Issue

Cite this: *Chem. Commun.*, 2016, 52, 10509

Received 28th June 2016,
Accepted 23rd July 2016

DOI: 10.1039/c6cc05395e

www.rsc.org/chemcomm

Why metal–oxos react with dihydroanthracene and cyclohexadiene at comparable rates, despite having different C–H bond strengths. A computational study†

Johannes E. M. N. Klein,*[a] Büsra Dereli,[b] Lawrence Que Jr.[a] and Christopher J. Cramer[b]

1,4-Cyclohexadiene (CHD) and 9,10-dihydroanthracene (DHA) are two substrates used to probe the steric requirements of metal–oxo oxidants in H-atom-transfer (HAT) reactions, based on the assumption that they have comparable C–H bond dissociation enthalpies (BDEs). We use computations to demonstrate that the BDE of DHA is ∼3.5 kcal mol^{-1} larger than that of CHD and that their often comparable reactivity is based on a competing interplay of bond strengths and favorable van der Waals interactions.

1,4-Cyclohexadiene (CHD) and 9,10-dihydroanthracene (DHA) are common substrates for the study of hydrogen-atom-transfer (HAT) reactivity involving nonpolar C–H bonds.[1] Their relatively high reactivities are primarily associated with the low bond dissociation enthalpies (BDEs) for their doubly allylic and benzylic C(sp^3)–H bonds, respectively. The C–H bond strengths in CHD and DHA are often judged to be similar and Luo[2] recommends BDE values for CHD and DHA of 76.0 ± 1.2[3] and 76.3[4] kcal mol^{-1}, respectively, based on various experimental measurements. Such a similarity in BDEs suggests that these two compounds may be used to probe the steric environment encountered by a C–H substrate in HAT reactions, with the expectation that both substrates would react at comparable rates when the metal-based oxidant or, more generally, the H-atom acceptor is sterically unencumbered. By contrast, a faster rate for the smaller CHD may be anticipated when the H-atom acceptor is less accessible. In computational studies of HAT reactions involving these two substrates, we found that the BDEs for these two substrates are predicted/computed to be rather different. This observation prompted us to reinvestigate their BDEs and to evaluate their respective reactivities in HAT reactions with three metal–oxo complexes (Fig. 1).

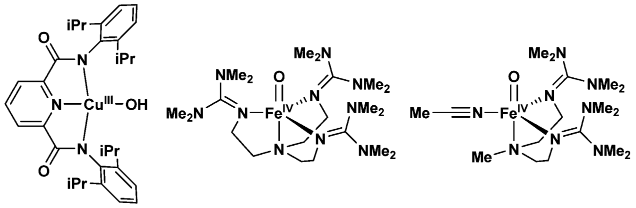
$Cu^{III}(OH)(L)$ $[Fe^{IV}(O)(TMG_3tren)]^{2+}$ $[Fe^{IV}(O)(TMG_2dien)(MeCN)]^{2+}$

Fig. 1 Metal–oxo complexes used in this study.

We first computed BDE values for CHD and DHA using the M06-2X[5] functional in combination with the def2-TZVPP[6] basis set. Benchmarking has demonstrated that the M06-2X functional can predict dissociation energies in radical generating reactions with a mean unsigned error of 1.8 kcal mol^{-1} over a data set of 61 examples.[7] At this level of theory, the BDEs for CHD (75.5 kcal mol^{-1}) and DHA (79.0 kcal mol^{-1}) are found to be different (Table 1), and by considerably more than the experimental error associated with the recommendations of Luo noted above. We note that the experimental BDE of CHD has been re-evaluated recently,[8] resulting in a value of 76.9 ± 0.7 kcal mol^{-1}, which agrees reasonably well with the M06-2X predicted value. A BDE difference of 3.5 kcal mol^{-1} would be expected to result in a noticeable difference in reactivity, and appears at first glance to be inconsistent with experimentally observed trends where these two substrates display similar reactivity in many instances (*vide infra*). These results suggest two potential scenarios: (a) the computed BDE values, and more importantly the difference between them, is not accurate or (b) the similar rates for HAT reactions with CHD and DHA do not arise from having similar BDEs but must involve other factors that counterbalance a substantial BDE difference. To address these possibilities, we carried out additional calculations of the BDEs of these compounds using wave function theory (WFT) methods and computed transition-state (TS) structures and associated energies of activation for the HAT reactions of both compounds with the three complexes in Fig. 1.

For an alternative computation of the BDEs of CHD and DHA, we computed energies using the *jun–jun* dual method of

---

[a] *Department of Chemistry and Center for Metals in Biocatalysis, University of Minnesota, 207 Pleasant St. S.E., Minneapolis, Minnesota 55455, USA. E-mail: kleinj@umn.edu*

[b] *Department of Chemistry, Supercomputing Institute, and Chemical Theory Center, University of Minnesota, 207 Pleasant Street S.E., Minneapolis, Minnesota 55455, USA*

† Electronic supplementary information (ESI) available: Full computational and experimental details, and coordinates for all structures. See DOI: 10.1039/c6cc05395e

Table 1 Computed BDE values for CHD and DHA[a]

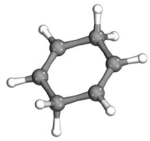

CHD

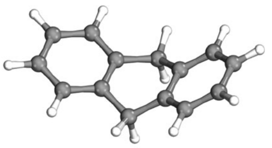

DHA

Compound	Computational method	BDE [kcal mol^{-1}]
CHD	M06-2X/def2-TZVPP	75.5
DHA	M06-2X/def2-TZVPP	79.0
CHD	*jun–jun*[b]	76.3
DHA	*jun–jun*[b]	79.9

[a] Structural depictions are based on geometries obtained at the M06-2X/def2-TZVPP level of theory. [b] E(*jun–jun*) ≈ E(CCSD(T)-F12a/jun-cc-pV(D+d)Z) + (E(MP2-F12/jun-cc-pV(T+d)Z) − E(MP2-F12/jun-cc-pV(D+d)Z)).[9]

Truhlar and co-workers, which can be considered an estimate for CCSD(T)/CBS (for details see ESI†).[9] The BDEs of CHD and DHA at the *jun–jun* level are 76.3 and 79.9 kcal mol^{-1}, respectively (Table 1). In addition to being in good agreement with M06-2X, and in essentially quantitative agreement with respect to the BDE difference, we expect these results to be close to chemical accuracy (note that the value predicted for CHD is within experimental error of the recent measurement of Gao *et al.*[8] mentioned above). Thus, we conclude that the similar reactivity of CHD and DHA observed for many HAT reactions is not attributable to similar BDEs but involves other effects that compensate for the difference in BDEs.

We now consider some specific examples of HAT reactions with CHD and DHA, beginning with $[\mathrm{Fe^{IV}(O)TMG_3tren}]^{2+}$[10] and $[\mathrm{Fe^{IV}(O)TMG_2dien(MeCN)}]^{2+}$[11] (Fig. 1). With the former, the rate of DHA oxidation is slower than that of CHD oxidation, which has been attributed to steric crowding associated with the TMG$_3$tren ligand. Removal of one of the side arms of the ligand reduces the crowding of the oxo unit in the latter, resulting in comparable and overall increased rates for the oxidation of both CHD and DHA. Experimental second order rate constants (k_2) are listed in Table 2 for comparison. We note here that both $[\mathrm{Fe^{IV}(O)TMG_3tren}]^{2+}$ and $[\mathrm{Fe^{IV}(O)TMG_2dien(MeCN)}]^{2+}$ belong to the rare subset of synthetic non-heme Fe^{IV}(O) complexes with an S = 2 ground state, which is enforced by the trigonal bipyramidal coordination geometry.[12] Most other such synthetic complexes possess an S = 1 ground state,[13] the HAT reactivity of which has been proposed to proceed on the S = 2 spin surface owing to two-state reactivity (TSR).[14] In the presently selected examples the complication of a change in spin state is alleviated. One aspect to consider, however, are the frontier molecular orbitals (FMOs) involved.[15] For S = 2 complexes a σ pathway has been proposed to be favorable, leading to a Fe–O–H(C) bond angle of ∼180° in the TS structure upon population of the empty $d\sigma_{z^2}{}^*$ orbital and resulting in a high spin (S = 5/2) Fe^{III}(OH) intermediate. A competing π pathway, in which one of the singly occupied $d\pi_{xz/yz}{}^*$ orbitals is populated, would lead to a bond angle of ∼120° in the transition state resulting in an intermediate spin (S = 3/2) Fe^{III}(OH) intermediate. The formation of a high-spin configuration is usually considered to be favorable and attributed to exchange-enhanced reactivity.[15b,c] For completeness we computed both pathways for the $[\mathrm{Fe^{IV}(O)TMG_2dien(MeCN)}]^{2+}$ complex. This also allows us to evaluate the role of the approach of the substrate. It should be noted that an alternative π pathway leading to a high spin configuration has been described recently but we do not consider that here.[16]

Table 2 Comparison of experimentally determined second order rate constants (k_2 in units of M^{-1} s^{-1}) of HAT from CHD and DHA for the complexes studied here computationally

Complex	CHD	DHA	Ref.
$[\mathrm{Fe^{IV}(O)TMG_3tren}]^{2+}$	1.2[a]	0.090[a]	10*a*
$[\mathrm{Fe^{IV}(O)TMG_2dien(MeCN)}]^{2+}$	18[a]	57[a]	11
Cu^{III}(OH)(L)	38[b,c]	50[b]	17*a*

[a] In MeCN at −30 °C. [b] In difluorobenzene at −25 °C. [c] Kindly measured by DD and WBT (see acknowledgements).

In addition to these Fe^{IV}(O) complexes we also include a Cu^{III}(OH)(L) complex (Fig. 1) that is capable of oxidizing nonpolar C–H bonds.[17] The challenge that we introduce with this particular complex arises from the closed-shell singlet configuration of the starting materials, which must transition to an open-shell configuration (broken symmetry within the context of single-configurational Kohn–Sham DFT)[18] along the reaction coordinate. To corroborate these calculations with experimental numbers we report in the present publication the second order rate constant (k_2) for the oxidation of CHD by the Cu^{III}(OH) complex, which allows us to make the desired comparison to the previously reported value for the oxidation of DHA; these values are in close agreement (Table 2).

So, we reiterate the questions that are raised by the computed BDEs: (i) what is the origin of the comparable reactivity? (ii) Can we use DHA and CHD to probe steric interactions between transition metal complexes and substrates?

When inspecting the structures of both CHD and DHA, an obvious structural difference becomes apparent (*cf.* Table 1). The CHD molecule is flat and possesses D_{2h} symmetry, whereas the DHA molecule is butterflied and exhibits C_{2v} symmetry. These computed structural features are in agreement with crystallographically determined parameters for these compounds.[19] To probe how these structural differences contribute to the BDE difference, we computed the enthalpy of activation for inversion of the DHA molecule *via* a D_{2h} symmetric transition state. We obtained a value of $\Delta H^{\ddagger}_{298}$ = 1.1 kcal mol^{-1} (M06-2X/def2-TZVPP), indicating that the geometrical change is likely a non-trivial contributor to the difference in BDE, but other factors must also be at least as important.

We did not expect a substantial difference with regards to steric interactions caused by the slight geometrical differences exhibited by the two substrates. We suspected instead that the difference in BDEs can be compensated for through favorable van der Waals interactions[20] (dispersion) between the oxidant and DHA that lower the activation energy for DHA to the same level as for CHD. We probed this hypothesis through a series of calculations where we first computed reaction paths using the B3LYP[21] functional, which poorly accounts for such weak interactions, and then compared these results to a set of calculations with the same functional including Grimme's D3[22] dispersion correction.

Such an approach was also recently reported by Wagner and Schreiner.[23] Solvation effects were taken into account through the COSMO[24] solvation model. Before going into details of the calculations, we note at this stage that the results here do not aim at an exact reproduction of the experimental values but rather are designed to allow us to understand the trends exhibited by experiment. The HAT reactions examined here exhibit non-classical kinetic isotope effects (KIEs), but we do not attempt to compute tunneling transmission coefficients as Shaik and co-workers have shown these to be very similar for CHD and DHA in general.[25] Therefore, we will discuss the differences of activation barriers ($\Delta\Delta G^{\ddagger}$) between CHD and DHA oxidation and not the absolute computed barrier heights, which are significantly influenced by the inclusion of Grimme's D3 dispersion correction (Table 3). The full computational details can be found in the ESI.†

In all calculations for the HAT reactions from CHD and DHA using the B3LYP functional, *i.e.*, in the absence of dispersion, we observe an energy difference of +4.1 to +6.2 kcal mol^{-1} with respect to the activation free energies for CHD *vs.* DHA oxidation. For the complexes $[\mathrm{Fe^{IV}(O)TMG_2dien(MeCN)}]^{2+}$ and $\mathrm{Cu^{III}(OH)(L)}$, differences of +4.1 to +5.1 kcal mol^{-1} roughly reflect the computed difference in BDE between CHD and DHA but are inconsistent with the experimental observation of similar rates for CHD and DHA oxidation (Table 2). The difference in the computed activation free energies for the $[\mathrm{Fe^{IV}(O)TMG_3tren}]^{2+}$ complex is a somewhat larger 6.2 kcal mol^{-1}, which may be attributed to the steric bulk of the TMG$_3$tren ligand. These energy gaps are roughly eliminated upon inclusion of Grimme's D3 dispersion correction. Indeed, with dispersion included, it is the HAT reaction from DHA that is computed to be slightly more favorable for $[\mathrm{Fe^{IV}(O)TMG_2dien(MeCN)}]^{2+}$ and $\mathrm{Cu^{III}(OH)(L)}$ by margins of $-1.8(\sigma)/-0.2(\pi)$ and -1.1 kcal mol^{-1}, respectively. The CHD barrier remains slightly lower than the one for DHA for the HAT reaction of the $[\mathrm{Fe^{IV}(O)TMG_3tren}]^{2+}$ complex. In all cases, the counterbalancing effects of BDE difference and dispersion lead to a consistent agreement between computations and experiment, although the Grimme D3 dispersion correction seems to slightly over-stabilize the DHA TS structures, a feature which has been documented in the literature before.[26] Notably, in the case of $[\mathrm{Fe^{IV}(O)TMG_2dien(MeCN)}]^{2+}$, the influence of dispersion on the differential activation free energies is of similar magnitude, independent of which pathway, σ or π, is followed. In Fig. 2, representative TS structures for the HAT reactions of CHD and DHA with $[\mathrm{Fe^{IV}(O)TMG_2dien(MeCN)}]^{2+}$ are depicted. Geometrical perturbations due to the inclusion of dispersion are small, and TS structures for the HAT reaction by the other complexes are quite similar (compare ESI†). This can also be extended to a similarity between the electronic structure of the TS structures for CHD and DHA oxidation. As depicted in Fig. 2, there is very little difference in the spin densities between the two substrates. However, the electronic structures associated with the reactions can be quite different for the complexes studied as evident from the spin density distributions (see ESI†), which further supports the generality of the observations made here. This set of calculations allows us to answer the originally posed questions as follows: (i) the comparable reactivity of CHD and DHA that is often observed experimentally is not a reflection of similar BDEs, but rather reflects a well-balanced interplay between BDE difference and dispersion interactions leading to an overall comparable rate in HAT reactions. (ii) Despite the difference in BDE computed here, the CHD–DHA-model can still serve to quantify the steric interactions between a given oxidant and the substrate. We recommend, however, referring to "comparable reactivity" rather than "similar BDEs" when exploiting their comparison in the future, as the former is a better reflection of the observed phenomenon and encompasses all effects that contribute to the reactivity of a given substrate rather than singling out the BDEs.

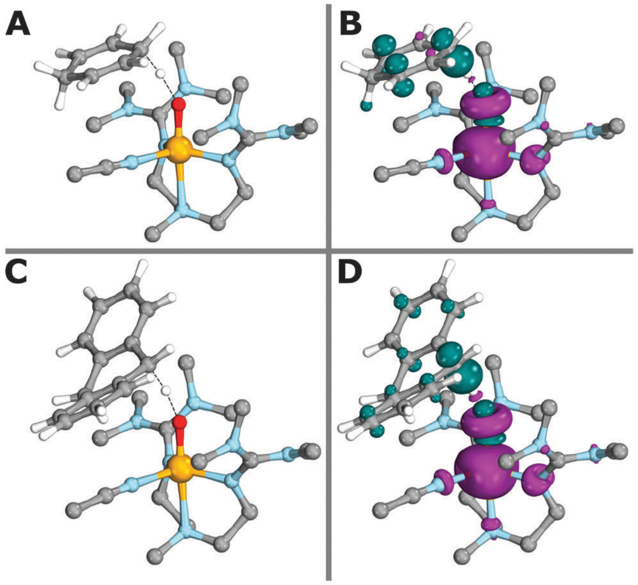

Fig. 2 Depictions of the transition states (B3LYP-D3/def2-SVP(Fe:def2-TZVP)/COSMO) (ε = 35.88) for HAT from CHD (A) and DHA (C) by the $[\mathrm{Fe^{IV}(O)TMG_2dien(MeCN)}]^{2+}$ complex and plots of the associated spin densities (B) and (D). Depictions were made using IboView[27] (isosurface 0.005). Ligand H-atoms are omitted for clarity.

Table 3 Comparison of computed activation free energies (kcal mol^{-1}) for HAT with and without dispersion correction[a]

Complex [dispersion correction]		$\Delta G^{\ddagger}_{298}$ [b] CHD	DHA	$\Delta\Delta G^{\ddagger}$ CHD *vs.* DHA
$[\mathrm{Fe^{IV}(O)TMG_3tren}]^{2+}(\sigma)$	[–]	23.1	29.3	+6.2
$[\mathrm{Fe^{IV}(O)TMG_3tren}]^{2+}(\sigma)$	[D3]	13.7	14.4	+0.7
$[\mathrm{Fe^{IV}(O)TMG_2dien(MeCN)}]^{2+}(\sigma)$	[–]	21.3	25.4	+4.1
$[\mathrm{Fe^{IV}(O)TMG_2dien(MeCN)}]^{2+}(\sigma)$	[D3]	12.7	10.9	−1.8
$[\mathrm{Fe^{IV}(O)TMG_2dien(MeCN)}]^{2+}(\pi)$	[–]	26.8	31.7	+4.9
$[\mathrm{Fe^{IV}(O)TMG_2dien(MeCN)}]^{2+}(\pi)$	[D3]	15.8	15.6	−0.2
$\mathrm{Cu^{III}(OH)(L)}$	[–]	22.6	27.6	+5.1
$\mathrm{Cu^{III}(OH)(L)}$	[D3]	12.0	10.9	−1.1

[a] Calculations were carried out at the B3LYP-def2-TZVPP/B3LYP-def2-SVP(Fe:def2-TZVP) level of theory. COSMO was used in all calculations. Grimme's dispersion correction (D3) was used where indicated. [b] Barriers are referenced to the fully dissociated reactants.

In summary, we have re-evaluated the BDEs for CHD and DHA computationally and found that the value for CHD, 76.3 (*jun–jun*) is in excellent agreement with the recently reported experimental value of 76.9 ± 0.7 kcal mol^{-1}.[8] We further find a value of 79.9 kcal mol^{-1} for DHA, which disagrees with the value of 76.3 kcal mol^{-1}[4] that is recommended by Luo in his extensive compilation of BDE values.[2] Future experimental re-evaluation of this BDE is strongly encouraged. We have further demonstrated, through computations of activation barriers for HAT reactions for representative transition metal complexes, that this discrepancy in BDEs does not necessarily impart a difference in reactivity between the compounds when participating as substrates in HAT reactions. Instead, increased dispersion for the larger DHA lowers its activation free energy when interacting with a "large but not too large" oxidant, resulting in an observation of similar reactivity to that of CHD. Previous comparisons made in the literature regarding the probing of steric interactions with DHA remain valid, but for more nuanced reasons.

J. E. M. N. K. thanks the Alexander von Humboldt Foundation for a Feodor Lynen Research Fellowship. For support of this work, we thank the National Science Foundation (CHE-1361595 to C. J. C., and CHE-1361773 to L. Q.). We thank Debanjan Dhar and William B. Tolman (University of Minnesota) for providing the second order rate constant of CHD oxidation by Cu^{III}(OH)L.

References

1 (*a*) X. Engelmann, I. Monte-Pérez and K. Ray, *Angew. Chem., Int. Ed.*, 2016, **55**, 7632–7649; (*b*) T. Matsumoto, K. Ohkubo, K. Honda, A. Yazawa, H. Furutachi, S. Fujinami, S. Fukuzumi and M. Suzuki, *J. Am. Chem. Soc.*, 2009, **131**, 9258–9267; (*c*) D. Wang, K. Ray, M. J. Collins, E. R. Farquhar, J. R. Frisch, L. Gomez, T. A. Jackson, M. Kerscher, A. Waleska, P. Comba, M. Costas and L. Que, Jr., *Chem. Sci.*, 2013, **4**, 282–291; (*d*) D. E. Lansky and D. P. Goldberg, *Inorg. Chem.*, 2006, **45**, 5119–5125; (*e*) R. E. Cowley, N. A. Eckert, S. Vaddadi, T. M. Figg, T. R. Cundari and P. L. Holland, *J. Am. Chem. Soc.*, 2011, **133**, 9796–9811; (*f*) W.-L. Man, W. W. Y. Lam, H.-K. Kwong, S.-M. Peng, W.-T. Wong and T.-C. Lau, *Inorg. Chem.*, 2010, **49**, 73–81.

2 Y.-R. Luo, *Comprehensive Handbook of Chemical Bond Energies*, CRC Press, Taylor & Francis Group, Boca Raton, FL, 2007.

3 W. Tsang, *J. Phys. Chem.*, 1986, **90**, 1152–1155.

4 S. E. Stein and R. L. Brown, *J. Am. Chem. Soc.*, 1991, **113**, 787–793.

5 Y. Zhao and D. Truhlar, *Theor. Chem. Acc.*, 2008, **120**, 215–241.

6 F. Weigend and R. Ahlrichs, *Phys. Chem. Chem. Phys.*, 2005, **7**, 3297–3305.

7 Y. Zhao and D. G. Truhlar, *J. Phys. Chem. A*, 2008, **112**, 1095–1099.

8 Y. Gao, N. J. DeYonker, E. C. Garrett, A. K. Wilson, T. R. Cundari and P. Marshall, *J. Phys. Chem. A*, 2009, **113**, 6955–6963.

9 (*a*) E. Papajak and D. G. Truhlar, *J. Chem. Phys.*, 2012, **137**, 064110; (*b*) J. Zheng, P. Seal and D. G. Truhlar, *Chem. Sci.*, 2013, **4**, 200–212.

10 (*a*) J. England, M. Martinho, E. R. Farquhar, J. R. Frisch, E. L. Bominaar, E. Münck and L. Que, Jr., *Angew. Chem., Int. Ed.*, 2009, **48**, 3622–3626; (*b*) J. England, Y. Guo, E. R. Farquhar, V. G. Young, Jr., E. Münck and L. Que, Jr., *J. Am. Chem. Soc.*, 2010, **132**, 8635–8644; (*c*) S. D. Wong, C. B. Bell, III, L. V. Liu, Y. Kwak, J. England, E. E. Alp, J. Zhao, L. Que, Jr and E. I. Solomon, *Angew. Chem., Int. Ed.*, 2011, **50**, 3215–3218.

11 J. England, Y. Guo, K. M. Van Heuvelen, M. A. Cranswick, G. T. Rohde, E. L. Bominaar, E. Münck and L. Que, Jr., *J. Am. Chem. Soc.*, 2011, **133**, 11880–11883.

12 M. Puri and L. Que, Jr., *Acc. Chem. Res.*, 2015, **48**, 2443–2452.

13 (*a*) A. R. McDonald and L. Que, Jr., *Coord. Chem. Rev.*, 2013, **257**, 414–428; (*b*) J. E. M. N. Klein and L. Que, Jr., Biomimetic High-Valent Mononuclear Nonheme Iron-Oxo Chemistry, in *Encyclopedia of Inorganic and Bioinorganic Chemistry (EIBC)*, ed. R. A. Scott, John Wiley, Chichester, 2016, DOI: 10.1002/9781119951438.eibc2344.

14 (*a*) D. Schröder, S. Shaik and H. Schwarz, *Acc. Chem. Res.*, 2000, **33**, 139–145; (*b*) S. Shaik, *Int. J. Mass Spectrom.*, 2013, **354–355**, 5–14.

15 (*a*) M. Srnec, S. D. Wong and E. I. Solomon, *Dalton Trans.*, 2014, **43**, 17567–17577; (*b*) H. Chen, W. Lai and S. Shaik, *J. Phys. Chem. Lett.*, 2010, **1**, 1533–1540; (*c*) S. Shaik, H. Chen and D. Janardanan, *Nat. Chem.*, 2011, **3**, 19–27.

16 (*a*) M. Srnec, S. D. Wong, M. L. Matthews, C. Krebs, J. M. Bollinger and E. I. Solomon, *J. Am. Chem. Soc.*, 2016, **138**, 5110–5122; (*b*) S. D. Wong, M. Srnec, M. L. Matthews, L. V. Liu, Y. Kwak, K. Park, C. B. Bell Iii, E. E. Alp, J. Zhao, Y. Yoda, S. Kitao, M. Seto, C. Krebs, J. M. Bollinger and E. I. Solomon, *Nature*, 2013, **499**, 320–323.

17 (*a*) D. Dhar and W. B. Tolman, *J. Am. Chem. Soc.*, 2015, **137**, 1322–1329; (*b*) D. Dhar, G. M. Yee, A. D. Spaeth, D. W. Boyce, H. Zhang, B. Dereli, C. J. Cramer and W. B. Tolman, *J. Am. Chem. Soc.*, 2016, **138**, 356–368; (*c*) N. Gagnon and W. B. Tolman, *Acc. Chem. Res.*, 2015, **48**, 2126–2131.

18 (*a*) F. Neese, *Coord. Chem. Rev.*, 2009, **253**, 526–563; (*b*) C. J. Cramer and D. G. Truhlar, *Phys. Chem. Chem. Phys.*, 2009, **11**, 10757–10816.

19 (*a*) A. Kupka, C. Schauerte and K. Merz, *Cryst. Growth Des.*, 2014, **14**, 2985–2989; (*b*) G. A. Jeffrey, J. Buschmann, C. W. Lehmann and P. Luger, *J. Am. Chem. Soc.*, 1988, **110**, 7218–7219.

20 (*a*) S. Grimme, *Wiley Interdiscip. Rev.: Comput. Mol. Sci.*, 2011, **1**, 211–228; (*b*) S. Grimme, A. Hansen, J. G. Brandenburg and C. Bannwarth, *Chem. Rev.*, 2016, **116**, 5105–5154.

21 (*a*) A. D. Becke, *J. Chem. Phys.*, 1993, **98**, 5648–5652; (*b*) C. Lee, W. Yang and R. G. Parr, *Phys. Rev. B: Condens. Matter Mater. Phys.*, 1988, **37**, 785–789.

22 S. Grimme, J. Antony, S. Ehrlich and H. Krieg, *J. Chem. Phys.*, 2010, **132**, 154104.

23 J. P. Wagner and P. R. Schreiner, *J. Chem. Theory Comput.*, 2016, **12**, 231–237.

24 A. Klamt and G. Schüürmann, *J. Chem. Soc., Perkin Trans. 2*, 1993, 799–805.

25 (*a*) D. Mandal, R. Ramanan, D. Usharani, D. Janardanan, B. Wang and S. Shaik, *J. Am. Chem. Soc.*, 2015, **137**, 722–733; (*b*) D. Mandal and S. Shaik, *J. Am. Chem. Soc.*, 2016, **138**, 2094–2097.

26 A. Hansen, C. Bannwarth, S. Grimme, P. Petrović, C. Werlé and J.-P. Djukic, *ChemistryOpen*, 2014, **3**, 177–189.

27 (*a*) G. Knizia, http://www.iboview.org/; (*b*) G. Knizia and J. E. M. N. Klein, *Angew. Chem., Int. Ed.*, 2015, **54**, 5518–5522.